Published in final edited form as:
Hear Res. 2005 June ; 204(1-2): 156–169. doi:10.1016/j.heares.2005.02.002.

Cytoplasmic and intra-nuclear binding of gentamicin does not require endocytosis

Sigrid E. Myrdal, **Katherine C. Johnson**, and **Peter S. Steyger**
Oregon Hearing Research Center, Oregon Health and Science University, 3181 SW Sam Jackson Park Road, Portland, Oregon, 97239

Abstract

Understanding the cellular mechanism(s) by which the oto- and nephrotoxic aminoglycoside antibiotics penetrate cells, and the precise intracellular distribution of these molecules, will enable identification of aminoglycoside-sensitive targets, and potential uptake blockers. Clones of two kidney cell lines, OK and MDCK, were treated with the aminoglycoside gentamicin linked to the fluorophore Texas Red (GTTR). As in earlier reports, endosomal accumulation was observed in live cells, or cells fixed with formaldehyde only. However, delipidation of fixed cells revealed GTTR fluorescence in cytoplasmic and nuclear compartments. Immunolabeling of both GTTR, and unconjugated gentamicin corresponded to the cytoplasmic distribution of GTTR fluorescence. Intra-nuclear GTTR binding co-localized with labeled RNA in the nucleoli and trans-nuclear tubules. Cytoplasmic and nuclear distribution of GTTR was quenched by phosphatidylinositol-bisphosphate (PIP_2), a known ligand for gentamicin. Cytoplasmic and nuclear GTTR binding increased over time (at 37°C, or on ice to inhibit endocytosis), and was serially competed off by increasing concentrations of unconjugated gentamicin, i.e. GTTR binding is saturable. In contrast, little or no reduction of endocytotic GTTR uptake was observed when cells were co-incubated with up to 4 mg/mL unconjugated gentamicin. Thus, cytoplasmic and nuclear GTTR uptake is time-dependent, weakly temperature-dependent and saturable, suggesting that it occurs via an endosome-independent mechanism, implicating ion channels, transporters or pores in the plasma membrane as bioregulatory routes for gentamicin entry into cells.

Keywords

gentamicin; aminoglycoside; non-endocytotic; cytoplasmic; drug uptake

Introduction

Aminoglycoside antibiotics continue to be important antibiotics in the treatment of tuberculosis and Gram-negative infections (Begg et al., 1995; de Jager et al., 2002), and in the prophylactic protection of burn victims and premature infants (Hall et al., 1986; Miller, 1985). Unfortunately, oto- and nephrotoxicity remain serious complications resulting from the clinical use of aminoglycosides.

Nephrotoxicity occurs in nearly 50% of patients treated for greater than 14 days (Leehey et al., 1993), resulting in increased morbidity during and after treatment, including organ failure and death (Hock et al., 1995; Leehey et al., 1993; van Lent-Evers et al., 1999). However,

Address correspondence to: Peter S. Steyger, Ph.D., Oregon Hearing Research Center, NRC04, Oregon Health & Science University, 3181 Sam Jackson Park Road, Portland, OR 97239 USA. FAX: (+1) 503-494-5656, Voice: (+1) 503-494-1062, E-mail: steygerp@ohsu.edu (preferred).

nephrotoxicity is often reversible following epithelial cell proliferation (Tulkens, 1989). The incidence of hearing loss approaches 20% of patients treated with aminoglycosides, and is permanent if inner ear sensory cells are lost (de Jager et al., 2002; Hall et al., 1986; Kahlmeter et al., 1984). Acute side effects of aminoglycosides can also compromise their therapeutic utility by inducing magnesium wasting (Kang et al., 2000; Quamme, 1986) and increased excretion of sodium, potassium, and chloride (Kidwell et al., 1994) through inhibition of ion reuptake in the distal portion of the nephron. Other side effects are respiratory paralysis and gastrointestinal disturbances resulting from inhibitory effects at the neuromuscular junction (Fiekers, 1983; Goldhill et al., 1996), analgesia of dorsal root ganglion sensory neurons (Zhou et al., 2002; Zhou et al., 2001), and a negative inotropic effect on cardiac myocytes (Belus et al., 2001; De la Chapelle-Groz et al., 1988).

Although the antibacterial activities of aminoglycosides are well understood, aminoglycoside toxicity in eukaryotic cells is not. Earlier efforts to identify the intracellular sites of aminoglycoside toxicity were made by determining the association of aminoglycosides with intracellular compartments, and by investigating the mechanism of aminoglycoside penetration into target cells. Results varied depending on the techniques used. Earlier electron microscopical studies showed the apparent uptake of the aminoglycoside gentamicin into the cytoplasmic compartments of kidney tubule cells (Gilbert et al., 1989; Wedeen et al., 1983). More recently, this distribution was suggested in immunocytochemical and fluorescence studies of inner ear hair cells (Hiel et al., 1992; Imamura et al., 2003; Steyger et al., 2003). Biochemical studies (using radioactive aminoglycosides) reported reduced gentamicin uptake in cells incubated at lower temperatures and that these residual levels of gentamicin represented plasmalemmal binding (Decorti et al., 1999; Williams et al., 1987b), although no microscopy was done to show spatial distribution.

Other recent reports describe endocytotic uptake of gentamicin in kidney cells (Beauchamp et al., 1991; Sandoval et al., 1998; Sandoval et al., 2000; Sandoval et al., 2002) and sensory hair cells (Aran et al., 1993; Hashino et al., 1997; Hiel et al., 1992). Endocytosed gentamicin is transported to Golgi bodies, endoplasmic reticuli and lysosomes (Hashino et al., 1997; Sandoval et al., 1998; Sandoval et al., 2000), and may subsequently be released into the cytoplasm (Sandoval et al., 2004).

In this study, we have used cultured immortal kidney cell lines as models for hair cells to facilitate comparisons among large numbers of specimens. Kidney epithelia share numerous characteristics with inner ear sensory hair cells. In addition to being pharmacologically-sensitive to aminoglycoside antibiotics, both sensory hair cells and kidney tubule cells are mechanosensors (Corey et al., 1983; Nauli et al., 2004), and express myosin VIIa, which has been implicated in aminoglycoside uptake (Richardson et al., 1997; Wolfrum et al., 1998). Both cell types are polarized epithelial cells, with tight junctions connecting adjoining cells, and expressing amiloride-sensitive and transient receptor potential channels (Bagger-Sjoback et al., 1988; Corey et al., 2004; Cortright et al., 2001; Ellison et al., 1987; Forge, 1985; Furness et al., 1996; Gonzalez-Mariscal et al., 2000; Harris et al., 2001; Jorgensen et al., 1988; Kuhn et al., 1975; Liedtke et al., 2000; Meyers et al., 2003; Strotmann et al., 2000; Tiedemann et al., 1983; Zheng et al., 2003). We used gentamicin conjugated to Texas Red (GTTR) determine if aminoglycosides can enter cells by non-endocytotic mechanisms, as for other fluorescent macromolecules (Corey et al., 2004; Gale et al., 2001; Hellwig et al., 2004; Meyers et al., 2003). We found saturable, GTTR binding within the cytoplasm and nucleus in fixed and delipidated cultured kidney cells. Binding was endosome-independent implicating ion channels, membrane transporters or pores as probable routes for gentamicin uptake into these compartments.

Materials and Methods

All materials were from Sigma-Aldrich (Saint Louis, MO), unless otherwise stated.

Conjugation

The conjugation of gentamicin to Texas Red (TR) succinimidyl esters (Molecular Probes, OR) was optimized with regard to time, temperature, pH, and ligand/reactive fluorophore ratio to maximize labeling efficiency and to minimize the possibility of over-labeling the gentamicin. This ensures the maintenance of the polycationic nature of gentamicin, which undoubtedly is required for its biological activity. After conjugation, the reaction mixture was separated by reversed phase chromatography using C-18 columns (Burdick and Jackson, Muskegon, MI) to isolate the conjugate and thereby eliminate competition from unconjugated gentamicin, or potential contamination by unreacted TR. The isolated GTTR conjugate is then aliquoted, dried, and stored dessicated, in the dark at −20°C until required.

Cell Culture

Canine kidney distal tubule (MDCK) cells were a gift from Dr. David Ellison (OHSU). Opossum proximal tubule-derived kidney cells (OK) were purchased from American Type Culture Collection (Manassas, VA). OKs and MDCKs were cultured in antibiotic-free minimal essential medium (MEM-α, Invitrogen, Carlsbad, CA) supplemented with 10% fetal bovine serum (FBS) at 37°C with 5% CO_2, 95% air. Complete medium for OK cells was also supplemented with insulin-transferrin-selenium (ITS) and interferon-γ (5 ng/mL). Plates used for OK cells were coated with 0.2% gelatin (in water) for 2 or more hours at 37°C. After draining, plates were treated at room temperature with a 0.9% saline solution containing 10% FBS and 10% rat-tail collagen (gift of Rosemarie Drake-Baumann, PhD, VA Medical Center, Portland, Oregon), and dried under sterile conditions. Plates were rinsed with complete medium just prior to use. For experimental specimens, cells were seeded into Nunc eight-well coverglass chambers (ISC BioExpress, Kaysville, UT) in complete medium, and after 3-5 days, both cell types were subconfluent, and MDCK cells had become columnar.

GTTR treatment

Subconfluent MDCK or OK cells were treated with 1 μg/mL of GTTR, in complete medium, for 2 hours at 37°C or on ice. (The amount of GTTR is expressed as the weight of the gentamicin moiety within the conjugate.) In competition experiments, MDCK cells were simultaneously treated with unconjugated gentamicin (up to 4 mg/mL) for 2 hours.

Fixation, delipidation, and washing

After treatment, cells were washed three times with complete medium and then immediately imaged live (see below; Fig. 2A), or fixed. Most fixation was done by treating cells with 4% formaldehyde and 0.5% Triton X-100 (FATX) in 0.1 M phosphate buffered saline (PBS) for 45 minutes at room temperature, and followed by extensive washing with PBS (4-6 times, or until foaming in suction pipette ceased) prior to imaging (Fig 2B). Alternatively, cells were fixed in 4% formaldehyde alone (FA), washed and imaged (Fig. 2C) prior to delipidation with 0.5% Triton X-100 in PBS, washed thoroughly and imaged again (Fig. 2D). Control cells were incubated with hydrolyzed TR (at the same concentration as the TR moiety in the GTTR experiments) and then imaged live, or fixed, delipidated, washed and then imaged.

PIP_2

To determine if cellular anionic phospholipids, like PIP_2, quenched GTTR fluorescence, MDCK cells in coverglass chambers were loaded with GTTR as described above. After fixation and delipidation using FATX, washing and imaging (Fig. 2B), cells were treated with 1 mg/

mL phosphatidylinositol-4,5-bisphosphate (PIP_2, Echelon Biosciences, Salt Lake City, UT) for 1.5 hours and re-imaged (Fig. 2E) prior to a second delipidation with 0.5% Triton, washing and imaging again (Fig. 2F).

Spectrophotometry

3-d scanning fluorescence spectroscopy of solutions containing TR or GTTR with or without PIP_2 were performed using a Safire fluorescence microplate reader (Tecan, Research Triangle Park, NC). GTTR (100 μg/mL; weight as gentamicin in molecule) and PIP_2 (155 μg/mL; approximately equimolar) were mixed vigorously in PBS solution and allowed to stand at room temperature for 1/2 hour prior to scanning. This was compared to the same concentration of GTTR alone in solution. Similar hydrolyzed TR solutions (at the same concentration as the Texas Red moiety in GTTR solutions), with or without PIP_2, were used as controls. Excitation and emission spectra were obtained over an excitation range of 570-604 nm (bandwidth 5 nm) and an emission range of 610-650 nm (bandwidth 5 nm).

Double-labeling with GTTR and Syto RNASelect

To determine if GTTR was co-localized with nuclear RNA, GTTR-loaded MDCK cells were methanol-fixed and labeled with Syto RNASelect (Molecular Probes, Eugene, OR). MDCK cells were grown on 8 well chambered coverslips to 40-50% confluency and incubated with GTTR (1 μg/mL) for 2 hours in complete supplemented medium at 37°C, 5% CO_2, 95% air. Cells were rinsed twice with PBS and fixed with ice-cold methanol only for 10 minutes on ice. Subsequently, cells were washed with PBS and incubated with 2 μM Syto RNASelect for 20 minutes, rinsed and observed using confocal microscopy.

Immunocytochemistry

To verify the co-distribution of GTTR fluorescence and gentamicin by immunocytochemistry, MDCK cells were grown on 8 well chambered coverslips to 40-50% confluency and incubated with GTTR (5 μg/mL) or unconjugated gentamicin (300 μg/mL) for 2 hours in complete medium, at 37°C or on ice. Cells were rinsed twice with PBS, fixed with 4% FA, rinsed 3 times with PBS, then permeabilized with ice-cold methanol for 5 minutes, and rinsed 3 times with PBS as described previously (Steyger et al., 2003). Cells were immunoblocked in 10% goat serum in PBS for 30 minutes and then incubated with 50 μg/mL rabbit anti-gentamicin antisera (American Quaalex, San Clemente, CA) for 1 hour. After washing with 1% goat serum in PBS, cells were further incubated with 20 μg/mL Alexa-488-conjugated goat-anti-rabbit antisera (Molecular Probes, Eugene, OR) for 45 minutes, washed, post-fixed with 4% FA for 15 minutes, and washed again. For immunocytochemical controls, untreated cells not exposed to GTTR or unconjugated gentamicin were fixed, permeabilized and immunoprocessed as for gentamicin- or GTTR-loaded cells. All wells were imaged using confocal microscopy.

Confocal Microscopy

Specimens were observed using a ×60 lens (N.A. 1.4), on a Nikon TE 300 inverted microscope (Melville, NY). Confocal images were collected on a Bio-Rad (Hercules, CA) MRC 1024 ES scanning laser system fitted with standard excitation and emission filters for Alexa-488/Syto RNASelect (excitation: 488 ± 12 nm; emission: 515 ± 10 nm) and Texas Red fluorophores (excitation: 568 ± 32 nm; emission: 620 ± 16 nm). Bio-Rad *.pic files acquired using Lasersharp 2000 software were exported as *.tif files and prepared for publication using Adobe Photoshop (v.7).

Semi-quantification

Each type of experiment was done multiple times ($n \geq 3$) to confirm trends. True quantification of optical sections from cultured cell layers is subject to intensity range variations between

experiments, as well within individual images. For this reason, representative images were chosen, and all comparative images were chosen from a single experiment. Intensity differences can often be best illustrated with a color lookup table, hot.lut, and a scale of 0-255 is shown in an intensity bar in Figure 6.

Results

Strategy

We chose the OK proximal tubule cell line because of the known clinical toxicity of aminoglycosides in the kidney proximal tubule (Fabrizii et al., 1997; Morin et al., 1984). Although far less subject to aminoglycoside-induced cell death, the MDCK distal tubule cell line was used because the distal tubule is subject to numerous acute effects (Kang et al., 2000; Kidwell et al., 1994; Quamme, 1986). Both were cloned from cultures that had been maintained for extended periods in the absence of the aminoglycoside streptomycin, a common bacterial prophylactic component of many culture media. This was done to optimize the response of cells to the aminoglycoside gentamicin. Although no morphological changes were observed in MDCK cells cultured without streptomycin, OK cells became morphologically and consistently more epitheloid after sustained culture (> 7 weeks) in streptomycin-free media (Fig. 1).

Intracellular Distribution of GTTR Uptake

In live MDCK cells treated with 1 μg/mL purified GTTR for 2 hours in complete medium at 37°C, we found GTTR fluorescence in a punctate, endosome-like distribution in live cells (Fig. 2A) similar to previous studies using Texas Red-conjugated gentamicin (Sandoval et al., 1998;Sandoval et al., 2000;Sandoval et al., 2002). Cells fixed with FA alone and imaged after washing with PBS exhibited the same vesicular labeling pattern (Fig. 2C).

However, when cells were fixed with FATX, no intracellular puncta of fluorescence were observed. Instead, GTTR was observed within the cytoplasm and at distinct intra-nuclear sites (Fig. 2B). In these fixed, delipidated cells, the cytoplasmic labeling reveals little substructure, but the intra-nuclear binding pattern was complex, showing round or ovoid structures, and also tubuloid structures traversing the nucleus (Fig. 2D). When FA-only fixed cells (Fig. 2C) were subsequently treated with 0.5% Triton X-100 (in PBS) alone, and washed with PBS, the punctate, endosome-like, fluorescence had disappeared and the cytoplasmic/nuclear fluorescence was visible (Fig. 2D). This suggests that cytoplasmic/nuclear GTTR was present, but not visible in live cells, or in cells fixed with FA only. It also suggests that penetration of GTTR into the cytoplasm was not an artifact of Triton X-100 being present during the fixation process.

Lipid Quenching of GTTR Fluorescence

When we observed fixed cells in FATX, or in Triton X-100 alone, GTTR fluorescence was significantly reduced (data not shown). Since Triton X-100, a surfactant used to remove cellular lipids, contains a lipid backbone, we reasoned that cellular lipids might be quenching GTTR fluorescence in live and FA-only fixed kidney cells. There are numerous reports of structural and functional associations of the polycationic gentamicin with cellular anionic phospholipids, and in particular with PIP_2 (Schacht, 1979; Williams et al., 1987a). To determine whether such an association might explain the lack of cytoplasmic/nuclear fluorescence in living or FA-only fixed cells, we attempted to quench GTTR fluorescence with PIP_2. Cells fixed with FATX and then rinsed (as in Fig 1B) were treated with 1 mg/mL PIP_2 and imaged while still in the PIP_2 solution (Fig. 2E). PIP_2 clearly quenched the GTTR fluorescence. This was not due to removal of the GTTR, because when the PIP_2-treated cells were again delipidated with 0.5% Triton

X-100 and washed, the GTTR fluorescence regained its former brightness and distribution (Fig.2F).

Reduction of GTTR fluorescence by PIP_2 was due to fluorescence quenching and not by excitation or emission spectral shifts. This was ascertained using 3-d scanning fluorescence spectroscopy of solutions containing TR or GTTR (100 μg/mL) with or without PIP_2 (155 μg/mL). Figure 3 (A-D) shows 3-d scans over an excitation range of 570-604 nm (bandwidth 5 nm) and an emission range of 610-650 nm (bandwidth 5 nm). No quenching was observed when PIP_2 was combined with TR in solution (Fig. 3B) compared with TR alone (Fig. 3A). PIP_2 in solution with GTTR exerted a quenching effect at all wavelengths (Fig. 3D) compared with GTTR alone (Fig. 3C). Using 2-d excitation scanning over a range of 290-604 with emission detected at 618 nm (Fig 2E) GTTR fluorescence was quenched in the presence of PIP_2. Using 2-d emission scanning over a range of 589-748 nm with excitation at 587 nm, GTTR emission was again quenched at all wavelengths in the presence of PIP_2. The quenching of GTTR (but not TR) fluorescence was probably due to binding of the amphipathic polyanion PIP_2 to the amphipathic polycation gentamicin, and alteration of electrons available to the fluorophore.

Label Specificity

MDCK cells treated with the same dose of hydrolyzed TR (based on fluorescence equivalent to GTTR in solution) exhibited fluorescently-labeled vesicles when imaged live (Fig. 2G), but not after FATX treatment (Fig. 2H). Thus, the gentamicin moiety of the GTTR conjugate is required for accumulation in the cytoplasmic/intra-nuclear compartment, but not in the endosomal compartment.

Intra-nuclear labeling

To determine if intra-nuclear GTTR labeling was co-localized with nuclear RNA, GTTR-loaded MDCK cells were fixed with methanol only, and labeled with Syto RNASelect. The globular intra-nuclear structures labeled by GTTR (Fig. 4A) were intensely co-labeled by Syto RNASelect (Fig. 4B,C), and are presumed to be nucleoli (Haugland et al., 2004). The trans-nuclear tubular structures were also co-labeled with both GTTR and Syto RNASelect (Fig. 4 insets). Unconjugated gentamicin (2 mg/mL) did not interfere with the binding of Syto RNASelect to nuclear material (data not shown). Cells incubated with GTTR (Fig. 4D) without subsequent Syto RNASelect treatment had negligible fluorescence at the 515 nm emission wavelength (Fig. 4E). Untreated cells fixed with methanol and labeled with fluorescent Syto RNASelect (515 nm emission; Fig. 4H) did not exhibit fluorescence bleed-through into the red (GTTR) channel (620 nm; Fig. 4G).

Characteristics of cytoplasmic and nuclear binding: Saturability, time and temperature effects

Saturability in the binding of a ligand demonstrates the existence of a limited number of binding sites and is the hallmark of specificity. Saturability is demonstrated if binding of a conjugated ligand can be serially reduced by increasing quantities of the native, unconjugated ligand. Such data also demonstrate that the conjugated ligand remains sufficiently bio-relevant that its distribution is a valid report of the distribution of the unconjugated molecule. Biological processes are time- and temperature-dependent, for example, crossing a barrier such as the plasma membrane. In particular, at low temperatures (cells held over ice) endosomal traffic would be halted but permeation through pores or ion channels could continue, albeit more slowly (Hille, 1992; Schaeffer et al., 1978).

Compartment Saturability

Both OK and MDCK cells were treated with GTTR at 1 μg/mL in complete culture medium for 2 hours at either 37°C or over ice. These cells were also treated with a dose range of 0 to 4000 μg/mL of unconjugated gentamicin. Cells were washed and imaged live (as in Fig. 2A), then fixed with FATX, and washed again with PBS prior to re-imaging (as in Fig. 2B). In live cells at 37°C, there was a large accumulation of GTTR-labeled puncta and this accumulation of endosome-like puncta was not visibly altered by even the highest doses of unconjugated gentamicin (Fig. 5, A5, inset). After FATX fixation and wash, cytoplasmic and nuclear fluorescence was observed in both cell types and at both temperatures (Fig. 5, A1, B1 and C1). Fluorescence was reduced in cells treated on ice, but, notably, still occurred (Fig. 5, B1, C1). At both temperatures and in both cell lines, increasing doses of unconjugated gentamicin serially reduced the amount of GTTR observed in both the cytoplasm and nucleoli (Fig. 5, A2-5, B2-5, and C2-5). Thus, cytoplasmic, but not endosomal, uptake of GTTR was saturable. Cells treated on ice and imaged live exhibited no endosome-like fluorescent puncta (Fig. 5, B1 inset). These results support two conclusions. Firstly, the cytoplasmic/nuclear compartment, but not the endosomal compartment, exhibited the characteristic of saturability that demonstrates specificity. This argues against the endosomal compartment being the source of the GTTR bound to the cytoplasmic/nuclear sites, either as a biological transit component or as a source for (artifactual) translocation during fixation. In addition, the saturable cytoplasmic uptake of GTTR by cells treated on ice demonstrates that gentamicin entry into the cytoplasmic compartment does not require endocytosis.

Time and Temperature

OK cells were treated with 1 μg/mL of GTTR in complete culture medium, at 37°C or on ice, for increasing time periods. Binding of GTTR within the cytoplasm and nucleus increased over time both at 37°C (Fig. 6 A1-6) and (more slowly) on ice (Fig 6, B1-6). At 37°C, cytoplasmic binding occurred prior to visible uptake into endosomes (Fig 6, compare A1-6 with insets, particular A2, and A3), consistent with Figure 5 showing that cytoplasmic uptake of GTTR does not require endocytosis. (Note that live images were acquired without washing out GTTR from the extracellular medium, so fluorescence is visible outside the cells.) No endosomes were observed on OK cells treated on ice for 2 hours (Fig. 6, B1 inset). GTTR was also taken up by MDCK cells as a function of time (data not shown). Increased binding over time at both temperatures reinforces the premise that cytoplasmic uptake of GTTR is a biological phenomenon and occurs in the absence of endocytosis.

Corroboration of GTTR distribution by immunocytochemistry

MDCK cells were loaded with GTTR or unconjugated gentamicin at 37°C; or on ice, for two hours, then fixed with FA only, permeabilized with methanol and immunolabeled with gentamicin antisera. At 37°C, GTTR fluorescence was observed throughout the cytoplasm, and as endosome-like puncta. In the nucleus, GTTR labeled the nucleoli and trans-nuclear tubules (Fig. 7A). Immunolabeling of GTTR with gentamicin antisera revealed close correlation with GTTR fluorescence including widespread diffuse cytoplasmic immunolabeling, and immunolabeling of GTTR-loaded vesicles (Fig. 7B,C). GTTR-labeled trans-nuclear tubules (Fig. 7A, inset) were also immunolabeled by gentamicin antisera (Fig. 7B, inset).

In cells loaded with GTTR on ice, extensive diffuse cytoplasmic GTTR fluorescence was observed, together with labeled trans-nuclear tubules (Fig. 7D and inset) that were also immunolabeled by gentamicin antisera (Fig. 7E). Endosome-like puncta of GTTR or immunolabeled GT fluorescence, observed in cells treated at 37°C, were absent in cells treated on ice (compare Fig. 7A with 7D, and Fig. 7B with 7E). Gentamicin antisera did not label GTTR-fluorescing nucleoli (Fig. 7B,E).

When MDCK cells were loaded with unconjugated gentamicin at 37°C (Fig. 7G) or on ice (Fig. 7H), diffuse immunofluorescence was observed in the cytoplasm and nucleoplasm, but excluded from nucleoli (as in immunolabeled GTTR specimens, Fig 7B,E), even at the higher gentamicin doses used here (300 μg/mL). Cells incubated with 5 μg/mL unconjugated gentamicin for 2 hours revealed similar but much weaker patterns of immunolabeling (data not shown). The distribution of immunolabeled GTTR and GT closely correlated with each other, and with the distribution of GTTR fluorescence (except for the nucleoli). These gentamicin immunolabeling patterns were not observed in gentamicin- or GTTR-loaded cells using antigen-adsorbed primary antibodies (data not shown); or in untreated cells (i.e., no GTTR or gentamicin loading), fixed and immunoprocessed with both primary and secondary antisera (Fig. 7I).

Discussion

GTTR as an Imaging Probe

The validity of our preparations of fluorescent GTTR as a biological tracer for gentamicin was demonstrated in Figure 5 that the fluorescent probe could be competed off its binding sites by unconjugated gentamicin. In this paper, purified GTTR is used as a probe to exhibit and validate a novel intracellular gentamicin distribution pattern. We examined both spatial distribution and intensity differences of GTTR in two kidney cell lines. The use of fluorescent ligands and confocal imaging offers considerable information regarding distribution of ligands in fixed specimens (neither sectioned nor fractionated). Instructive and reproducible differences in fluorescence intensity can be observed within an image or between images subjected to different experimental conditions. Fluorescent microscopy images of biological specimens are subject to natural variation among cells, especially at high resolution, making numerical intensity comparisons difficult to validate. It is more instructive to be able to *see* "clearly more", "clearly less", or "fairly similar" fluorescence for quantitative comparisons. Intensity differences as the result of experimental conditions are visually clear, and provide the phenomenological information for the conclusions of this study. For these reasons, we have not added numbers to our images, nor graphed intensity differences.

Cytoplasmic Penetration

This report describes a more rapid uptake of fluorescently-conjugated gentamicin throughout the cytoplasm and at intra-nuclear sites than previously described (Sandoval et al., 1998; Sandoval et al., 2004; Sandoval et al., 2000). Finding gentamicin in the cytoplasm is consistent with earlier studies using radiolabeling or biochemical extraction (Ding et al., 1995; Ding et al., 1997; Wedeen et al., 1983). Recent fluorescence and immunocytochemical studies in fixed, methanol-permeabilized frog saccular explants also showed gentamicin localization in vesicles, in the cytoplasm and the nucleus (Steyger et al., 2003). The cytoplasmic distribution of gentamicin is also consistent with studies in which gentamicin was able to override premature stop codons during (cytoplasmic) mRNA-protein translation in specific genetic diseases, e.g., cystic fibrosis (Bedwell et al., 1997; Clancy et al., 2001; Clemens et al., 2001; Keeling et al., 2002; Schulz et al., 2002). However, penetration of gentamicin directly into the cytoplasm and nucleus in the absence of endocytosis (i.e. cells held over ice) is contrary to recent reports describing gentamicin-Texas Red uptake by endocytosis, and subsequent release into the cytoplasm from vesicular compartments (Sandoval et al., 2004).

Cytoplasmic and nuclear GTTR fluorescence could not be seen in live cells in our studies (Fig. 1, B1 and B2) or in previous reports (Dunn et al., 2003), but only after both fixation and detergent delipidation as described here, and elsewhere (Sandoval et al., 2004). Probably the most important difference between our studies and earlier reports using fluorescently conjugated gentamicin is the degree of "permeabilization" used (Sandoval et al., 1998;

Sandoval et al., 2004; Sandoval et al., 2000; Sandoval et al., 2002). In those studies, Triton X-100 was used at a concentration of 0.05-0.1% for 10 minutes. In our studies, a 0.5% concentration was used for at least 30 minutes, and then thoroughly rinsed, thus more effectively removing cellular lipids. In addition, Sandoval et al. (1998, 2000, 2004) used much higher doses of fluorescent gentamicin, often by two-three orders of magnitude.

In earlier studies using the kidney cell line LLC-PK1, Sandoval et al. (1998) observed vesicular uptake of Texas Red-conjugated gentamicin, but not of the unconjugated Texas Red molecule. In our studies, the same dose of hydrolyzed TR (as that in GTTR) resulted in fluorescently-labeled vesicles in live cells (Fig. 2G), which was not seen after FATX treatment (Fig. 2H). This suggests non-specific endocytotic uptake of hydrolyzed TR (and by implication GTTR). However, since hydrolyzed TR did not label the cytoplasmic and nuclear domains, the gentamicin moiety of the GTTR conjugate was required for accumulation in those domains. This was further demonstrated by cold inhibition of endocytosis, during which cytoplasmic uptake of gentamicin still occurred (Figs. 5 and 7), as with FM1-43 in sensory hair cells, implicating ion channels as a mechanism of fluorophore uptake (Meyers et al., 2003).

Fluorescence Quenching

Triton X-100 and PIP_2 reduced the fluorescence of GTTR. The TR molecule is known to exhibit little change in fluorescence emission in response to environmental conditions, such as changes in pH (Haugland et al., 1996), although its fluorescence can be self-quenched at high concentrations. We also find no reports of environmental sensitivity when TR is conjugated to large molecules, such as antibodies (Haugland et al., 1996; Haugland et al., 2004). However, gentamicin, a mixture of 3 isoforms with an average MW of 469, is a polyamine, with 2 or 3 amine side groups remaining after conjugation with TR. Deprotonation of these amines alters the fluorescent emission (measured by fluorimetry) of TR covalently attached to the gentamicin compared to unconjugated TR in solution (unpublished studies). In both confocal imaging and fluorimetry, however, both excitation and emission wavelengths are selected with band-pass filters, so do not distinguish between (apparent) fluorescence quenching and an environmentally-induced spectral shift in the excitation or emission spectrum (or both). Such shifts could produce peaks that would miss the band pass filters and appear as quenching even if emission were enhanced at a different wavelength. However, spectral scans of GTTR in solution with or without PIP_2 over an excitation range of 290-609 nm and emission range of 598-750 nm produced 2- or 3-dimensional fluorescence maps which showed clearly that PIP_2 attenuated GTTR fluorescence at all wavelengths (Figure 3). PIP_2 had no effect on TR alone in solution, indicating that PIP_2 was interacting with the gentamicin moity of GTTR. Yet, in those experiments and in Figure 2 A3, PIP_2 did not completely block GTTR fluorescence, although almost no GTTR fluorescence was observed in live cells treated at temperatures incompatible with endosomal uptake. In solution, much higher concentrations of PIP_2 might have completely blocked fluorescence. In vivo, other lipids (e.g., phosphidylserines etc) or cellular quenching mechanisms may be involved. Additionally, PIP_2 may not bind as effectively to intracellular GTTR that had been cross-linked, via one or more of its amine groups as it can with free GTTR, which has 2 or 3 pendant amine groups in solution.

Intra-nuclear labeling

Gentamicin is known to bind to the major groove of prokaryotic and eukaryotic ribosomal RNA, a major component of nucleoli and ribosomes (Lynch et al., 2001; Yoshizawa et al., 1998). GTTR was co-localized with the RNA-specific Syto RNASelect fluorophore in intra-nuclear structures, identified as nucleoli (Haugland et al., 2004). In addition, the trans-nuclear tubular structures were also co-labeled with both Syto RNASelect and GTTR, suggesting that these sites were also rich in RNA as well as other gentamicin binding sites.

Characteristics of GTTR Accumulation into the Cytoplasmic Compartment

With either the proximal OK or distal MDCK kidney cell lines, binding of GTTR was time and temperature dependent, and saturable at both cytoplasmic and intra-nuclear sites. GTTR binding serially decreased as a function of increasing concentrations of unconjugated gentamicin in the culture media. Competition with the native molecule shows that intracellular gentamicin binding sites are limited in number, and that the conjugated molecule retains the biological characteristics of the native molecule, at least with regard to uptake and distribution (GTTR is a tracer, and would not be used to study toxicity or other physiological activities). This demonstrated the biological specificity of GTTR binding at these sites. At 37°C, we also observed vesicular uptake of GTTR over time. Unlike one previous, unconfirmed, report (Sandoval et al., 1998), we were unable, in numerous experiments, to see any significant reduction in vesicular uptake of GTTR, even using high excesses of native gentamicin (> 4000×). A possible explanation for this difference is that extended gentamicin treatment (1 mg/mL) of a porcine kidney tubule cell line (LLC PK1) inhibits endocytosis (Kempson et al., 1989). Thus the 12 mg/mL dose of gentamicin used in earlier studies LLC PK1 cells (Sandoval et al., 1998) could have reduced endocytotic uptake of Texas Red-conjugated gentamicin in a non-competitive manner. When OK and MDCK cells were treated with 4 mg/mL gentamicin for 2 hours, we observed only flattening of cells, which slightly altered the apparent distribution of vesicles, so a small decrease in vesicle number would be difficult to observe or document. In contrast, vesicular uptake of GTTR was little changed, unlike the near extinction of cytoplasmic and nuclear binding of GTTR at the highest doses of unconjugated gentamicin. This suggests that a large fraction of the vesicular uptake is associated with non-specific, fluid-phase endocytosis, since it is not saturable, confirming a previous report (Decorti et al., 1999). This non-specific endocytotic uptake of aminoglycosides is also consistent with the observation that GTTR within the vesicular compartment is only weakly associated with endosomal (or membranous) components during aldehyde fixation and is ultimately washed away during detergent permeabilization (see Figure 2). Furthermore, hydrolyzed Texas Red alone was seen only in vesicles of live cells, but it was not seen in the cytoplasmic or nuclear compartments after FATX treatment (Fig. 2).

Endocytosis of GTTR was not visibly reduced at a 4000-fold excess of competing unconjugated gentamicin, yet GTTR fluorescence in the cytoplasmic and nuclear compartments was greatly reduced. Cytoplasmic GTTR fluorescence was also observed in cells treated on ice to inhibit endocytosis. Inhibition of endocytosis in cells treated on ice was verified by live imaging of GTTR-loaded cells incubated on ice, and by the absence of endosome-like fluorescent puncta of GTTR or immunolabeling. In cells treated on ice, increasing concentrations of unconjugated gentamicin also serially reduced cytoplasmic and nuclear GTTR fluorescence. Taken together, these data strongly negate the possibility that GTTR released from endosomes during FATX treatment are the source of cytoplasmic and nuclear GTTR fluorescence.

Corroboration of GTTR distribution by immunocytochemistry

At 37°C, after FA fixation and methanol treatment, GTTR-loaded cells displayed both diffuse and punctate (vesicular) cytoplasmic fluorescence for both GTTR and immunolabeled GTTR, Gentamicin antibodies also co-localized with GTTR-labeled trans-nuclear tubules. In cells loaded with GTTR on ice, no punctate GTTR or immunolabeling could be observed, however, diffuse cytoplasmic and nucleoplasmic GTTR and immunofluorescence were both visible. GTTR-labeled nucleoli were negligibly immunolabeled. Immunocytochemical detection of unconjugated gentamicin loaded into cells on ice (and at 37°C) also correlated with the diffuse cytoplasmic distribution of both GTTR and immunolabeled GTTR. Thus, immunodetection of gentamicin or GTTR display similar distributions pattern as GTTR (except for nucleoli), demonstrating that fluorescence of GTTR was due to the gentamicin-Texas Red conjugate, and not due to cleaved TR molecules. The specific, high affinity binding of the gentamicin

molecule (or moiety) to RNA may lead to steric hindrance or immunogenic site masking and account for the negligible immunolabeling of nucleoli by gentamicin antisera. Indeed, GTTR labeling of the nucleoli may indicate one advantage of the GTTR conjugate over immunodetection of gentamicin because it eliminates the potential masking of immunogenic sites when gentamicin is specifically bound to intracellular ligands (e.g., RNA). The binding of GTTR to nucleoli (ribosomal RNA) is not surprising considering the known association of gentamicin with ribosomal RNA that induces protein mistranslation (Loveless et al., 1984; Lynch et al., 2001; Yoshizawa et al., 1998)

Significance

GTTR does not fluoresce within the cytoplasm of live cells. This illustrates an additional pitfall when attaching fluorophores to small molecules. The chemical nature of the molecule itself can influence the fluorescence of the attached fluorophore. In the case of GTTR, the electron densities of the basic amine groups on the gentamicin molecule were apparently modified while interacting with the acidic phospholipids (or other charged molecules) within the cytoplasm of live cells in a manner that reduced the fluorescence efficiency of the Texas Red moiety. This effect is undoubtedly largely responsible for the difference between our findings and other studies using fluorescence imaging of GTTR. In this report, we have shown biorelevant, non-endocytotic uptake of gentamicin, with cytoplasmic and intra-nuclear binding sites. Continued evaluation of these binding sites will elucidate the intracellular targets that mediate the biological and toxicological effects of aminoglycosides. Bullfrog saccular and murine cochlear hair cells also show cytoplasmic and nuclear distributions of GTTR uptake (Steyger et al., 2003; Steyger et al., 2004; Steyger et al., 2005) similar to the distributions seen in kidney tubule cells. Further investigation into the mechanisms of GTTR uptake into the cytoplasmic and nuclear compartments have suggested new methods for clinically reducing non-endocytotic aminoglycoside uptake, and potentially toxicity, in both kidney tubule cells and inner ear sensory cells (Myrdal et al., 2004; Myrdal et al., 2005; Steyger et al., 2004; Steyger et al., 2005)(manuscript in preparation).

Acknowledgments

We are grateful to Dr. David Ellison for the gift of MDCK cells, and for valuable consultations in these studies. These studies were funded by National Institute of Deafness and other Communication Disorders grants 04555 and 06084, with equipment grants from the American Foundation for Alternatives to Animal Research, and the Northwest Health Foundation. Portions of this work were presented in abstract form at the 27th Annual Midwinter Meeting of the Association for Research in Otolaryngology, Daytona Beach, February 2004.

References

Aran JM, Dulon D, Hiel H, Erre JP, Aurousseau C. Ototoxicity of aminosides: recent results on uptake and clearance of gentamycin by sensory cells of the cochlea. Rev Laryngol Otol Rhinol 1993;114:125–8.

Bagger-Sjoback D, Engstrom B, Hillerdal M. Membrane specializations in the human organ of Corti. Acta Otolaryngol (Stockh) 1988;106:19–28. [PubMed: 3421096]

Beauchamp D, Gourde P, Bergeron MG. Subcellular distribution of gentamicin in proximal tubular cells, determined by immunogold labeling. Antimicrob Agents Chemother 1991;35:2173–9. [PubMed: 1803988]

Bedwell DM, Kaenjak A, Benos DJ, Bebok Z, Bubien JK, Hong J, Tousson A, Clancy JP, Sorscher EJ. Suppression of a CFTR premature stop mutation in a bronchial epithelial cell line. Nat Med 1997;3:1280–4. [PubMed: 9359706]

Begg EJ, Barclay ML. Aminoglycosides--50 years on. Br J Clin Pharmacol 1995;39:597–603. [PubMed: 7654476]

Belus A, White E. Effects of antibiotics on the contractility and Ca2+ transients of rat cardiac myocytes. Eur J Pharmacol 2001;412:121–6. [PubMed: 11165223]

Clancy JP, Bebok Z, Ruiz F, King C, Jones J, Walker L, Greer H, Hong J, Wing L, Macaluso M, Lyrene R, Sorscher EJ, Bedwell DM. Evidence that systemic gentamicin suppresses premature stop mutations in patients with cystic fibrosis. Am J Respir Crit Care Med 2001;163:1683–92. [PubMed: 11401894]

Clemens PR, Duncan FJ. Progress in gene therapy for Duchenne muscular dystrophy. Curr Neurol Neurosci Rep 2001;1:89–96. [PubMed: 11898504]

Corey DP, Hudspeth AJ. Kinetics of the receptor current in bullfrog saccular hair cells. J Neurosci 1983;3:962–76. [PubMed: 6601694]

Corey DP, Garcia-Anoveros J, Holt JR, Kwan KY, Lin SY, Vollrath MA, Amalfitano A, Cheung EL, Derfler BH, Duggan A, Geleoc GS, Gray PA, Hoffman MP, Rehm HL, Tamasauskas D, Zhang DS. TRPA1 is a candidate for the mechanosensitive transduction channel of vertebrate hair cells. Nature 2004;432:723–730. [PubMed: 15483558]

Cortright DN, Crandall M, Sanchez JF, Zou T, Krause JE, White G. The tissue distribution and functional characterization of human VR1. Biochem Biophys Res Commun 2001;281:1183–9. [PubMed: 11243859]

de Jager P, van Altena R. Hearing loss and nephrotoxicity in long-term aminoglycoside treatment in patients with tuberculosis. Int J Tuberc Lung Dis 2002;6:622–7. [PubMed: 12102302]

De la Chapelle-Groz B, Athias P. Gentamicin causes the fast depression of action potential and contraction in cultured cardiocytes. Eur J Pharmacol 1988;152:111–20. [PubMed: 3208827]

Decorti G, Malusa N, Furlan G, Candussio L, Klugmann FB. Endocytosis of gentamicin in a proximal tubular renal cell line. Life Sci 1999;65:1115–24. [PubMed: 10503927]

Ding D, Jin X, Zhao J. Accumulation sites of kanamycin in cochlear basal membrane cells. Zhonghua Er Bi Yan Hou Ke Za Zhi 1995;30:323–5. [PubMed: 8762517]

Ding D, Jin X, Zhao J. Accumulation sites of kanamycin in the organ of Corti by microautoradiography. Zhonghua Er Bi Yan Hou Ke Za Zhi 1997;32:348–9. [PubMed: 10743109]

Dunn KW, Sandoval RM, Molitoris BA. Intravital imaging of the kidney using multiparameter multiphoton microscopy. Nephron Exp Nephrol 2003;94:e7–11. [PubMed: 12806182]

Ellison DH, Velazquez H, Wright FS. Mechanisms of sodium, potassium and chloride transport by the renal distal tubule. Miner Electrolyte Metab 1987;13:422–32. [PubMed: 3320724]

Fabrizii V, Thalhammer F, Horl WH. Aminoglycoside-induced nephrotoxicity. Wien Klin Wochenschr 1997;109:830–5. [PubMed: 9454436]

Fiekers JF. Effects of the aminoglycoside antibiotics, streptomycin and neomycin, on neuromuscular transmission. II. Postsynaptic considerations. J Pharmacol Exp Ther 1983;225:496–502. [PubMed: 6306208]

Forge A. Outer hair cell loss and supporting cell expansion following chronic gentamicin treatment. Hear Res 1985;19:171–82. [PubMed: 4055536]

Furness DN, Hackney CM, Benos DJ. The binding site on cochlear stereocilia for antisera raised against renal Na+ channels is blocked by amiloride and dihydrostreptomycin. Hear Res 1996;93:136–46. [PubMed: 8735075]

Gale JE, Marcotti W, Kennedy HJ, Kros CJ, Richardson GP. FM1-43 dye behaves as a permeant blocker of the hair-cell mechanotransducer channel. J Neurosci 2001;21:7013–25. [PubMed: 11549711]

Gilbert DN, Wood CA, Kohlhepp SJ, Kohnen PW, Houghton DC, Finkbeiner HC, Lindsley J, Bennett WM. Polyaspartic acid prevents experimental aminoglycoside nephrotoxicity. J Infect Dis 1989;159:945–53. [PubMed: 2651534]

Goldhill JM, Rose K, Percy WH. Effects of antibiotics on epithelial ion transport in the rabbit distal colon in-vitro. J Pharm Pharmacol 1996;48:651–6. [PubMed: 8832503]

Gonzalez-Mariscal L, Namorado MC, Martin D, Luna J, Alarcon L, Islas S, Valencia L, Muriel P, Ponce L, Reyes JL. Tight junction proteins ZO-1, ZO-2, and occludin along isolated renal tubules. Kidney Int 2000;57:2386–402. [PubMed: 10844608]

Hall JW 3rd, Herndon DN, Gary LB, Winkler JB. Auditory brainstem response in young burn-wound patients treated with ototoxic drugs. Int J Pediatr Otorhinolaryngol 1986;12:187–203. [PubMed: 3570684]

Harris DC, Wang Y, Campbell D. Regulation of tubular cell MCP-1 production by intracellular ions: a role for sodium and calcium. Exp Nephrol 2001;9:205–13. [PubMed: 11340305]

Hashino E, Shero M, Salvi RJ. Lysosomal targeting and accumulation of aminoglycoside antibiotics in sensory hair cells. Brain Res 1997;777:75–85. [PubMed: 9449415]

Haugland, RP.; Spence, MTZ.; Johnson, ID. Handbook of fluorescent probes and research chemicals. Vol. 6th. Molecular Probes; Eugene, OR, USA (4849 Pitchford Ave., Eugene 97402): 1996.

Haugland, RP.; Gregory, J.; Spence, MTZ.; Johnson, ID. Handbook of fluorescent probes and research chemicals. Vol. 9th. Molecular Probes; Eugene, OR, USA (4849 Pitchford Ave., Eugene 97402): 2004. online version

Hellwig N, Plant TD, Janson W, Schafer M, Schultz G, Schaefer M. TRPV1 acts as proton channel to induce acidification in nociceptive neurons. J Biol Chem 2004;279:34553–61. [PubMed: 15173182]

Hiel H, Schamel A, Erre JP, Hayashida T, Dulon D, Aran JM. Cellular and subcellular localization of tritiated gentamicin in the guinea pig cochlea following combined treatment with ethacrynic acid. Hear Res 1992;57:157–65. [PubMed: 1733909]

Hille, B. Ionic channels of excitable membranes. Sinauer Associates; Sunderland, Mass: 1992.

Hock R, Anderson RJ. Prevention of drug-induced nephrotoxicity in the intensive care unit. J Crit Care 1995;10:33–43. [PubMed: 7757141]

Imamura, SI.; Adams, JC. J Assoc Res Otolaryngol. 2003. Distribution of Gentamicin in the Guinea Pig Inner Ear after Local or Systemic Application. (in press), First Online JARO web site

Jorgensen F, Ohmori H. Amiloride blocks the mechano-electrical transduction channel of hair cells of the chick. J Physiol (Lond) 1988;403:577–88. [PubMed: 2473197]

Kahlmeter G, Dahlager JI. Aminoglycoside toxicity - a review of clinical studies published between 1975 and 1982. J Antimicrob Chemother 1984;13:9–22. [PubMed: 6365884]

Kang HS, Kerstan D, Dai L, Ritchie G, Quamme GA. Aminoglycosides inhibit hormone-stimulated Mg2 + uptake in mouse distal convoluted tubule cells. Can J Physiol Pharmacol 2000;78:595–602. [PubMed: 10958159]

Keeling KM, Bedwell DM. Clinically relevant aminoglycosides can suppress disease-associated premature stop mutations in the IDUA and P53 cDNAs in a mammalian translation system. J Mol Med 2002;80:367–76. [PubMed: 12072912]

Kempson SA, Ying AL, McAteer JA, Murer H. Endocytosis and Na+/solute cotransport in renal epithelial cells. J Biol Chem 1989;264:18451–6. [PubMed: 2572593]

Kidwell DT, McKeown JW, Grider JS, McCombs GB, Ott CE, Jackson BA. Acute effects of gentamicin on thick ascending limb function in the rat. Eur J Pharmacol 1994;270:97–103. [PubMed: 8157087]

Kuhn K, Reale E. Junctional complexes of the tubular cells in the human kidney as revealed with freeze-fracture. Cell Tissue Res 1975;160:193–205. [PubMed: 1149116]

Leehey DJ, Braun BI, Tholl DA, Chung LS, Gross CA, Roback JA, Lentino JR. Can pharmacokinetic dosing decrease nephrotoxicity associated with aminoglycoside therapy. J Am Soc Nephrol 1993;4:81–90. [PubMed: 8400072]

Liedtke W, Choe Y, Marti-Renom MA, Bell AM, Denis CS, Sali A, Hudspeth AJ, Friedman JM, Heller S. Vanilloid receptor-related osmotically activated channel (VR-OAC), a candidate vertebrate osmoreceptor. Cell 2000;103:525–35. [PubMed: 11081638]

Loveless MO, Kohlhepp SJ, Gilbert DN. The influence of aminoglycoside antibiotics on the in vitro function of rat liver ribosomes. J Lab Clin Med 1984;103:294–303. [PubMed: 6693798]

Lynch SR, Puglisi JD. Structure of a eukaryotic decoding region A-site RNA. J Mol Biol 2001;306:1023–35. [PubMed: 11237616]

Meyers JR, MacDonald RB, Duggan A, Lenzi D, Standaert DG, Corwin JT, Corey DP. Lighting up the senses: FM1-43 loading of sensory cells through nonselective ion channels. J Neurosci 2003;23:4054–65. [PubMed: 12764092]

Miller, JJ. Handbook of ototoxicity. CRC Press; Boca Raton: 1985.

Morin JP, Fillastre JP, Olier B. Antibiotic nephrotoxicity. Chemioterapia 1984;3:33–40. [PubMed: 6100174]

Myrdal SE, Steyger PS. TRPV1 Channel Mediates Gentamicin Entry In Cultured Kidney Cells. ARO Midwinter Meeting Abstracts 2004;27:135.

Myrdal SE, Steyger PS. TRPV1 Regulators Mediates Gentamicin Entry In Cultured Kidney Cells. Hearing Research. 2005submitted

Nauli SM, Zhou J. Polycystins and mechanosensation in renal and nodal cilia. Bioessays 2004;26:844–56. [PubMed: 15273987]

Quamme GA. Renal handling of magnesium: drug and hormone interactions. Magnesium 1986;5:248–72. [PubMed: 3543513]

Richardson GP, Forge A, Kros CJ, Fleming J, Brown SD, Steel KP. Myosin VIIA is required for aminoglycoside accumulation in cochlear hair cells. J Neurosci 1997;17:9506–19. [PubMed: 9391006]

Sandoval R, Leiser J, Molitoris BA. Aminoglycoside antibiotics traffic to the Golgi complex in LLC-PK1 cells. J Am Soc Nephrol 1998;9:167–74. [PubMed: 9527392]

Sandoval RM, Molitoris BA. Gentamicin traffics retrograde through the secretory pathway and is released in the cytosol via the endoplasmic reticulum. Am J Physiol Renal Physiol 2004;286:F617–24. [PubMed: 14625200]

Sandoval RM, Dunn KW, Molitoris BA. Gentamicin traffics rapidly and directly to the Golgi complex in LLC-PK(1) cells. Am J Physiol Renal Physiol 2000;279:F884–90. [PubMed: 11053049]

Sandoval RM, Bacallao RL, Dunn KW, Leiser JD, Molitoris BA. Nucleotide depletion increases trafficking of gentamicin to the Golgi complex in LLC-PK1 cells. Am J Physiol Renal Physiol 2002;283:F1422–9. [PubMed: 12388419]

Schacht J. Isolation of an aminoglycoside receptor from guinea pig inner ear tissues and kidney. Arch Otorhinolaryngol 1979;224:129–34. [PubMed: 226045]

Schaeffer SF, Raviola E. Membrane recycling in the cone cell endings of the turtle retina. J Cell Biol 1978;79:802–25. [PubMed: 730768]

Schulz A, Sangkuhl K, Lennert T, Wigger M, Price DA, Nuuja A, Gruters A, Schultz G, Schoneberg T. Aminoglycoside pretreatment partially restores the function of truncated V(2) vasopressin receptors found in patients with nephrogenic diabetes insipidus. J Clin Endocrinol Metab 2002;87:5247–57. [PubMed: 12414899]

Steyger PS, Peters SL, Rehling J, Hordichok A, Dai CF. Uptake of gentamicin by bullfrog saccular hair cells in vitro. J Assoc Res Otolaryngol 2003;4:565–78. [PubMed: 14605921]

Steyger PS, Spencer N, Hordichok AJ, Raphael RM, Myrdal SE. Reduction of Gentamicin Uptake in Hair Cells in vitro. ARO Midwinter Meeting Abstracts 2004;27:135.

Steyger, PS.; Razdan, PS.; Spencer, N.; Hordichok, AJ.; Johnson, K. Further evidence for aminoglycoside-permissive cation channels in inner ear explants; ARO Midwinter Meeting Abstracts; 2005. p. 27in press

Strotmann R, Harteneck C, Nunnenmacher K, Schultz G, Plant TD. OTRPC4, a nonselective cation channel that confers sensitivity to extracellular osmolarity. Nat Cell Biol 2000;2:695–702. [PubMed: 11025659]

Tiedemann K, Zaar K. The pig mesonephros. II. The proximal tubule: SEM, TEM and freeze-fracture images. Anat Embryol (Berl) 1983;168:241–52. [PubMed: 6660564]

Tulkens PM. Nephrotoxicity of aminoglycoside antibiotics. Toxicol Lett 1989;46:107–23. [PubMed: 2650018]

van Lent-Evers NA, Mathot RA, Geus WP, van Hout BA, Vinks AA. Impact of goal-oriented and model-based clinical pharmacokinetic dosing of aminoglycosides on clinical outcome: a cost-effectiveness analysis. Ther Drug Monit 1999;21:63–73. [PubMed: 10051056]

Wedeen RP, Batuman V, Cheeks C, Marquet E, Sobel H. Transport of gentamicin in rat proximal tubule. Lab Invest 1983;48:212–23. [PubMed: 6337301]

Williams SE, Zenner HP, Schacht J. Three molecular steps of aminoglycoside ototoxicity demonstrated in outer hair cells. Hear Res 1987a;30:11–8. [PubMed: 3680049]

Williams SE, Smith DE, Schacht J. Characteristics of gentamicin uptake in the isolated crista ampullaris of the inner ear of the guinea pig. Biochem Pharmacol 1987b;36:89–95. [PubMed: 3801057]

Wolfrum U, Liu X, Schmitt A, Udovichenko IP, Williams DS. Myosin VIIa as a common component of cilia and microvilli. Cell Motil Cytoskeleton 1998;40:261–71. [PubMed: 9678669]

Yoshizawa S, Fourmy D, Puglisi JD. Structural origins of gentamicin antibiotic action. Embo J 1998;17:6437–48. [PubMed: 9822590]

Zheng J, Dai C, Steyger PS, Kim Y, Vass Z, Ren T, Nuttall AL. Vanilloid receptors in hearing: altered cochlear sensitivity by vanilloids and expression of TRPV1 in the organ of corti. J Neurophysiol 2003;90:444–55. [PubMed: 12660354]

Zhou Y, Zhao ZQ. Effects of neomycin on high-threshold Ca(2+) currents and tetrodotoxin-resistant Na (+) currents in rat dorsal root ganglion neuron. Eur J Pharmacol 2002;450:29–35. [PubMed: 12176105]

Zhou Y, Zhou ZS, Zhao ZQ. Neomycin blocks capsaicin-evoked responses in rat dorsal root ganglion neurons. Neurosci Lett 2001;315:98–102. [PubMed: 11711224]

Abbreviations

FA
: 4% formaldehyde

FATX
: 4% formaldehyde plus 0.5% Triton X-100

FBS
: Fetal bovine serum

GT
: gentamicin

GTTR
: gentamicin conjugated to Texas Red

LLC-PK1
: Porcine kidney cell line derived from proximal tubule

MDCK
: Madin-Darby canine kidney cell line derived from distal tubule

N.A
: Numerical aperture

OK
: Opossum kidney cell line derived from proximal tubule

PBS
: Phosphate buffered saline

PIP_2
: phosphatidylinositol-4,5-bisphosphate

TR
: Texas Red

α-GT
: primary antibody against gentamicin

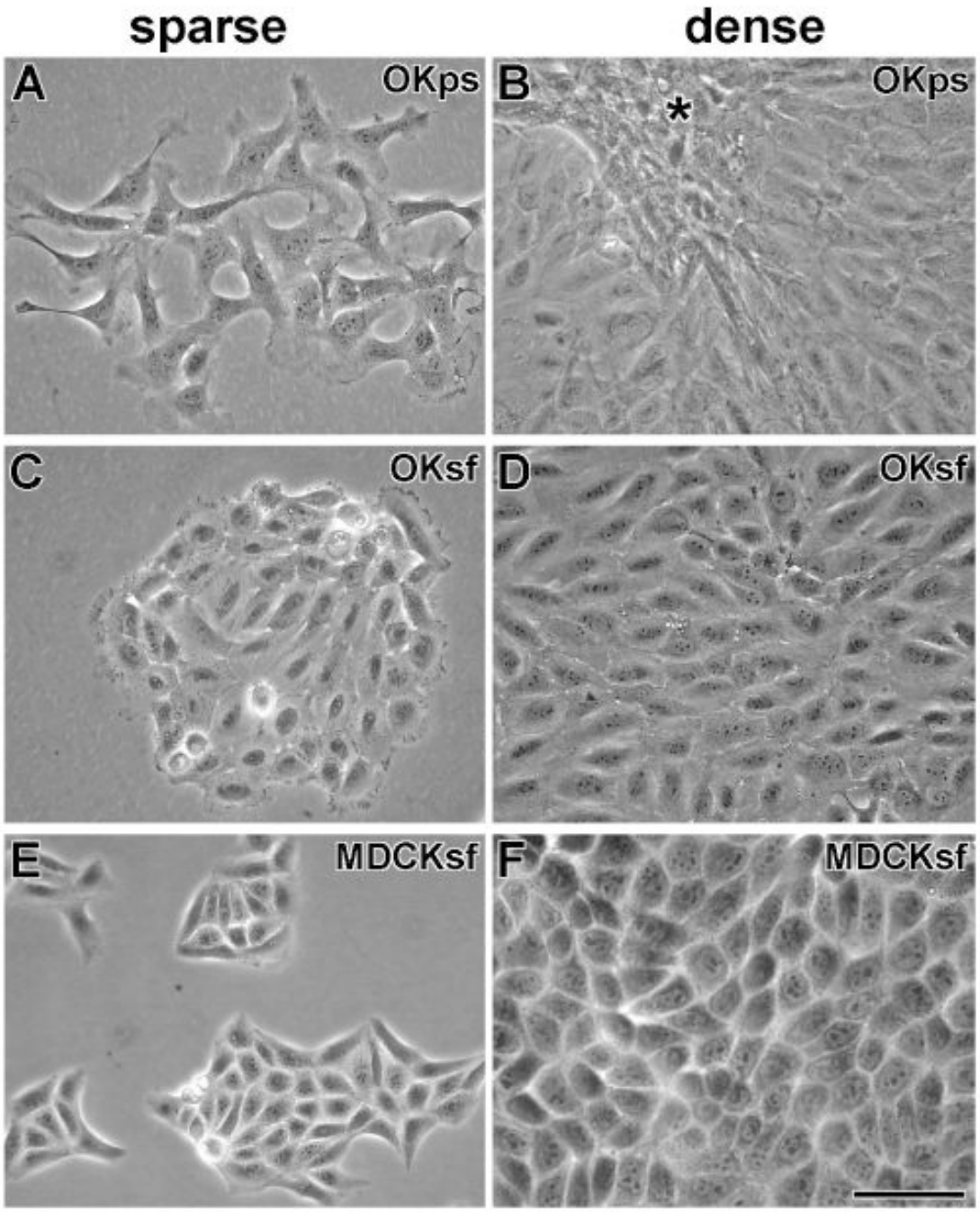

Figure 1. Morphology of OK and MDCK cells in complete medium with or without streptomycin

A). At low density, OK cells raised in penicillin-streptomycin culture media (OKps) look fibroblastic. B) At high density, OKps cells retain a fibroblastic morphology and crowd together (*). C) At low density, OK cells, grown in streptomycin-free media (OKsf) for at least 7 weeks, cluster together and have an epitheloid appearance. D) At high density, confluent OKsf cells retain their epitheloid appearance. E) At low density, MDCK cells, grown in streptomycin-free media for at least 7 weeks (MDCKsf), cluster together and appear epitheloid (as in penicillin-streptomycin media). F) At high density, confluent MDCKsf cells retain their epitheloid appearance. Scale bar = 50 μm.

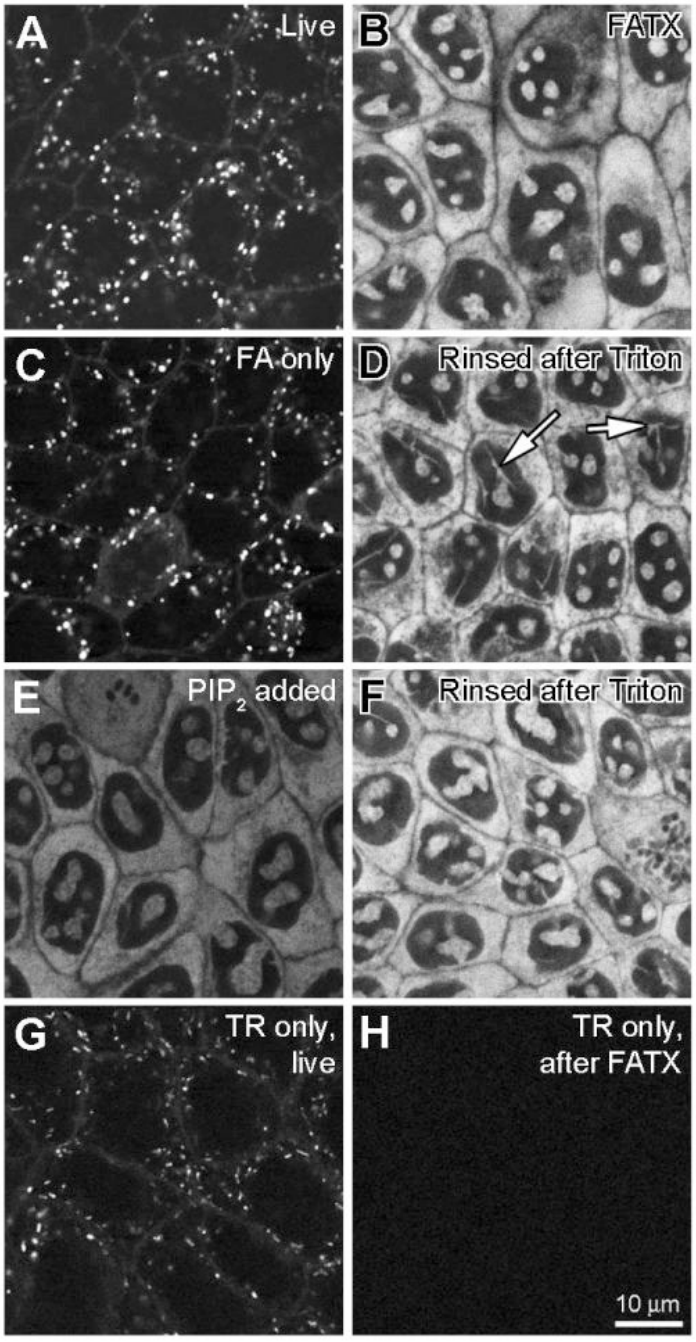

Figure 2. Cytoplasmic and intra-nuclear binding of Texas Red-conjugated gentamicin (GTTR)

MDCK cells were treated with 1 μg/mL GTTR at 37°C for 2 hours, washed and treated as described, then imaged using confocal microscopy. Control cells were treated identically with equivalent amounts of unconjugated, hydrolyzed Texas Red. All images were obtained using the same imaging parameters. A) Live cells with numerous GTTR-loaded vesicles. B) Cells washed after fixation with FATX show fluorescent cytoplasmic and intra-nuclear labeling, but no punctate (vesicular) GTTR fluorescence. C) Cells in 4% formaldehyde alone (FA) show vesicular and surface labeling. D) Cells fixed with FA and washed (as in C), then delipidated with 0.5% Triton X-100 and washed show bright cytoplasmic and intra-nuclear labeling, as in B). Arrows show fluorescent structures traversing the nucleus. E) Cells fixed with FATX (as

in B) treated with 1 mg/mL PIP_2 for 1.5 hours show quenched fluorescence. F) Cells treated with PIP_2 (as in E) then delipidated with 0.5 Triton X-100 and rinsed show recovery of fluorescence brightness. G) Live cells treated with TR alone and imaged have TR-loaded vesicles. H) Cells treated with TR, then fixed in FATX buffer and washed have no cytoplasmic or nuclear fluorescence.

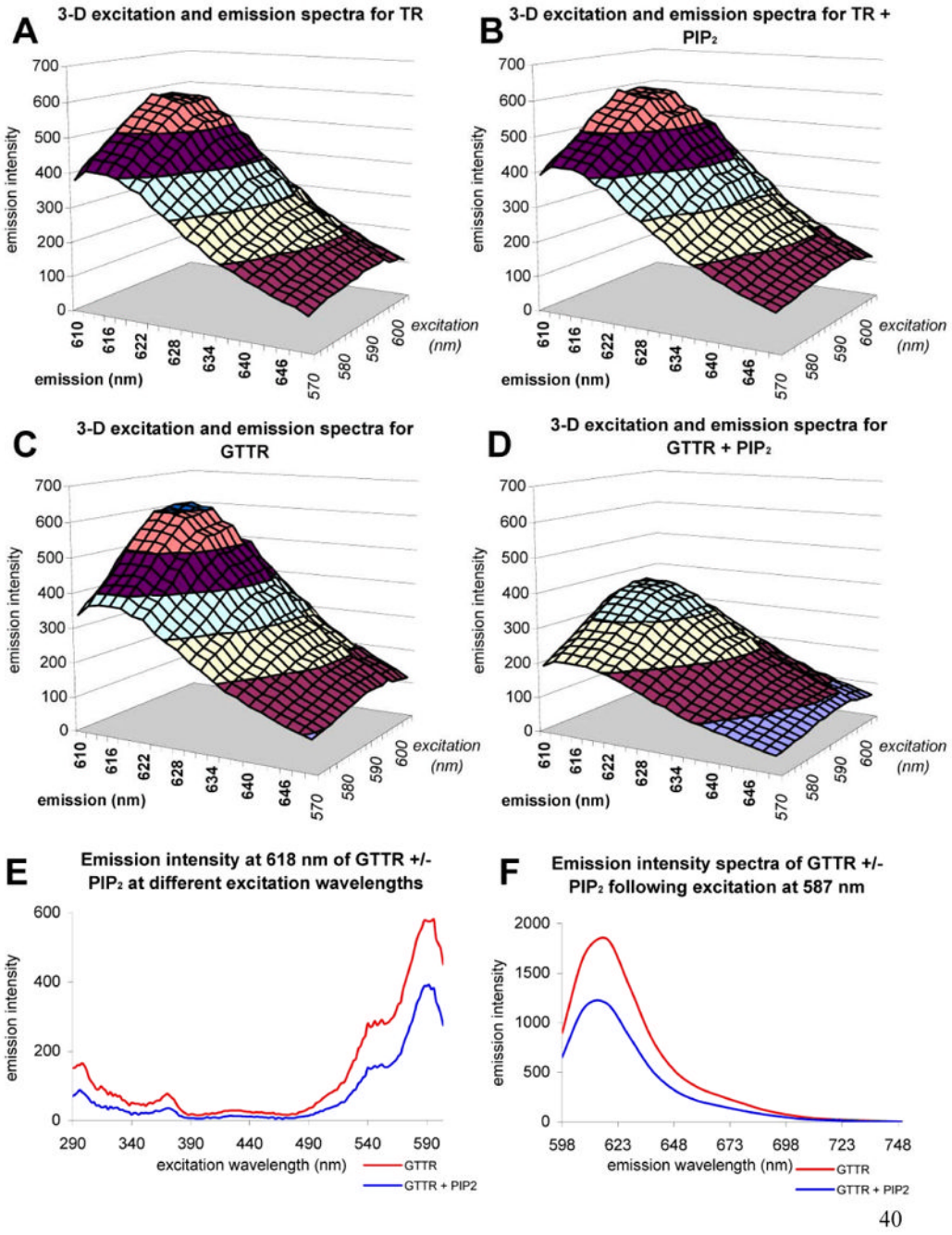

Figure 3. PIP_2 quenching of GTTR but not TR fluorescence

A-D) 3-dimensional excitation and emission scans; excitation 570-640 nm, emission 610-650 nm, bandwidth = 5 nm, emission intensity in arbitrary fluorescent units. A) Texas Red. B) Texas Red in the presence of PIP_2. Note the similarity of the spectra to that seen in A). C) GTTR. D) GTTR in the presence of PIP_2. Note the reduced fluorescence emission intensities compared to C). E) Emission scan of GTTR at 618 nm (bandwidth = 5 nm) in the absence (red) or presence (blue) of PIP_2 over the excitation wavelength range 290-604 nm. F) Emission scan of GTTR at the fixed excitation wavelength 587 nm (bandwidth = 5 nm) over the emission wavelength range 598 – 748 nm (bandwidth = 5 nm) in the absence (red) or presence (blue) of PIP_2.

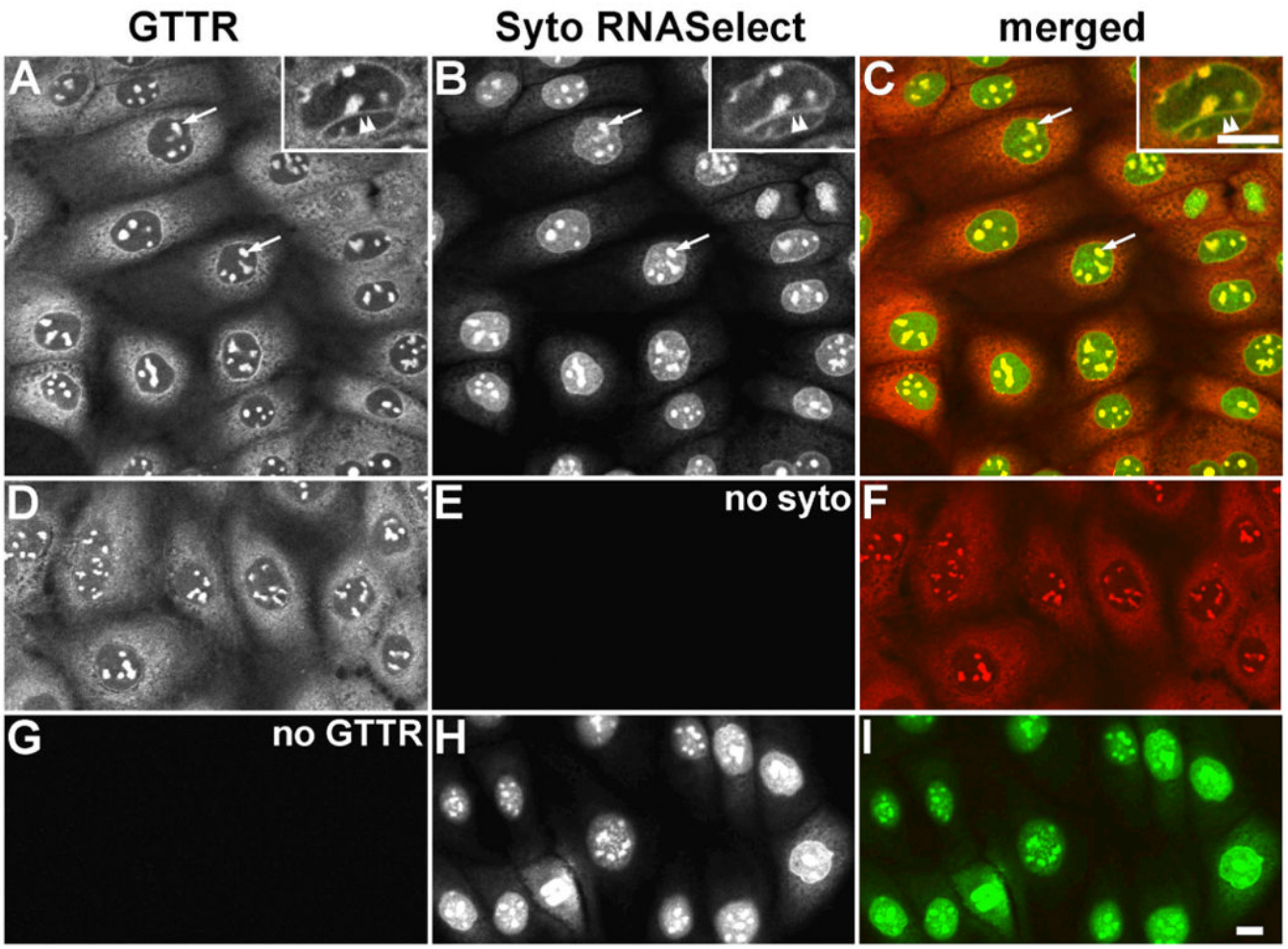

Figure 4. Distribution of GTTR in methanol-fixed MDCK cells double-labeled with Syto RNASelect

A) GTTR is diffusely distributed throughout the cytoplasm, and strongly labels the intra-nuclear structures (arrows), and trans-nuclear tubules (double arrowhead in inset). B) Syto RNASelect strongly labels the globular intra-nuclear structures (arrows), and trans-nuclear tubules (double arrowhead in inset). C) Merged images of (A) and (B), show co-localization of both GTTR and SYTO RNASelect fluorophores as yellow in globular intra-nuclear structures (arrows), and trans-nuclear tubules (double arrowhead in inset). D) Fluorescent GTTR-loaded cells. E) Cells in (D), not treated with Syto RNASelect, display negligible non-specific 515 nm fluorescence. F) Merged image of (D) and (E). G) Cells treated with SytoRNA Select only (in H) display no bleed-through fluorescence in red (GTTR) channel. H) Cells treated with Syto RNASelect. Note mitotic figure lower left. I) Merged image of (G) and (H). Scale bars = 10 μm.

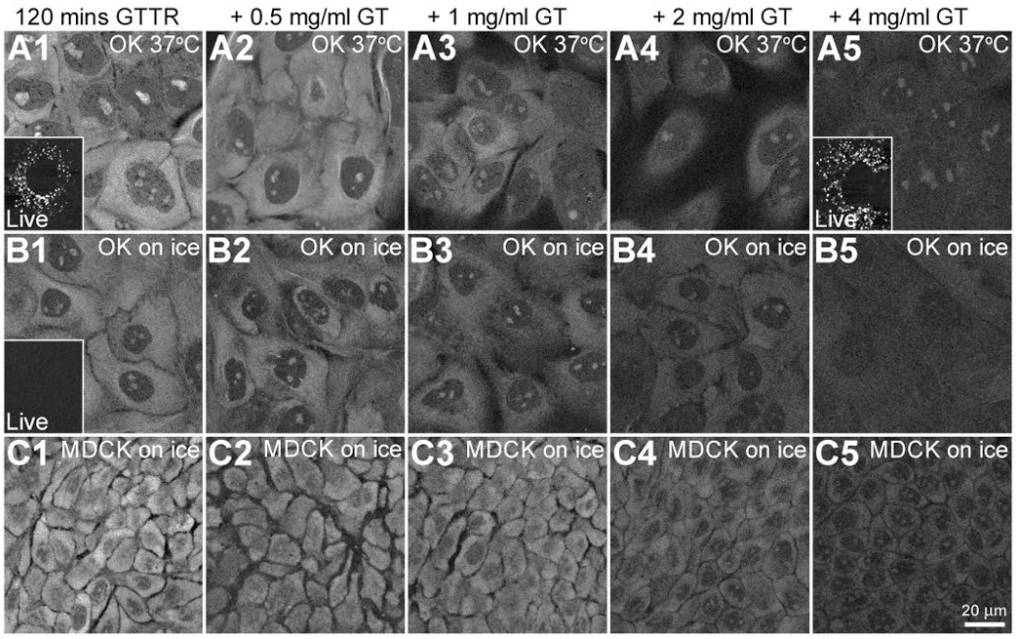

Figure 5. Saturability of cytoplasmic, but not vesicular GTTR fluorescence

OK or MDCK cells were treated with 1 μg/mL GTTR for 120 minutes at 37°C or held over ice in the presence of increasing concentrations of unconjugated gentamicin. Cells were imaged live or fixed with FATX and washed before imaging. A1-A5) At 37°C, OK cells, treated with GTTR show serially reduced labeling with increasing unconjugated gentamicin (GT) concentrations. Inset in A1) shows only vesicular GTTR labeling in live OK cells treated with GTTR alone. Inset in A5) also shows little or no decrease in vesicular GTTR labeling in live OK cells treated with GTTR plus 4 mg/mL unconjugated gentamicin. B1-B5) OK cells on ice show reduced GTTR binding in the cytoplasm and intra-nuclear compartments (compared to 37°C, A1-A5) and reduction of binding with increasing concentrations of unconjugated gentamicin concentrations. Inset in B1) shows no vesicular GTTR uptake in OK cells on ice when imaged live. C1-C5) MDCK cells on ice also show decreasing cytoplasmic GTTR fluorescence as concentration of unconjugated gentamicin increases.

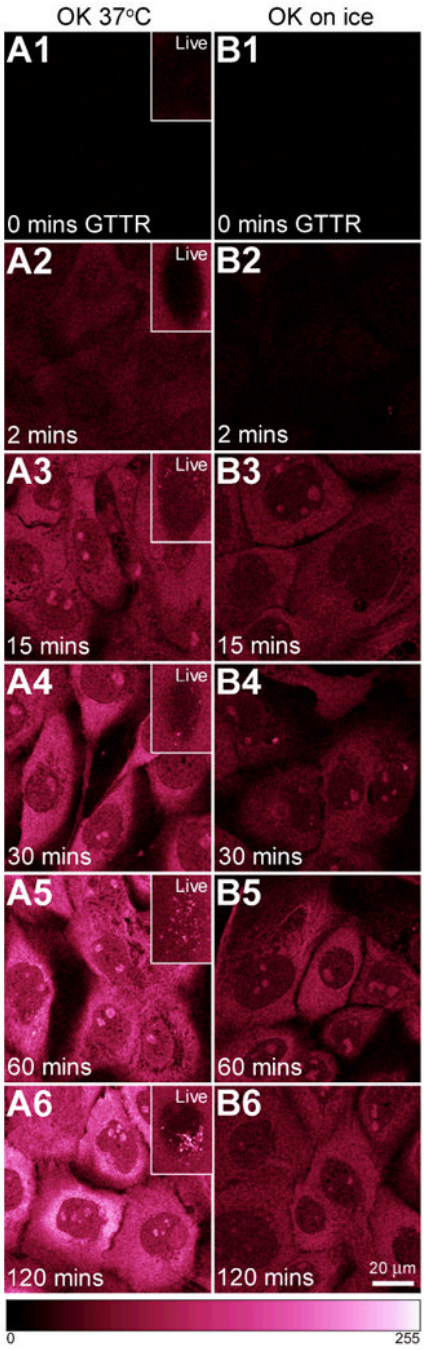

Figure 6. Influence of time and temperature on GTTR binding

OK cells were treated with 1 μg/mL GTTR at 37°C or on ice and imaged live (insets) or fixed after specified time intervals. A1-A6) Cells at 37°C show increasing cytoplasmic GTTR binding over time. Insets show cells imaged live, and endocytotic uptake 15 minutes (or later) after GTTR application. B1-B6) Cells held over ice during treatment show increased GTTR binding over time, but less intensely than that seen at 37°C. Scale bar = 20 μm. Color gradient at base represents fluorescent intensity from the hot.lut lookup table: 0 (no fluorescence, black) to 255 (saturated pixels, white), and enhances the ability of the human eye to discriminate intensity differences over grayscale images. Note live images in insets were acquired without washing out GTTR from the extracellular medium, so fluorescence is visible outside the cells.

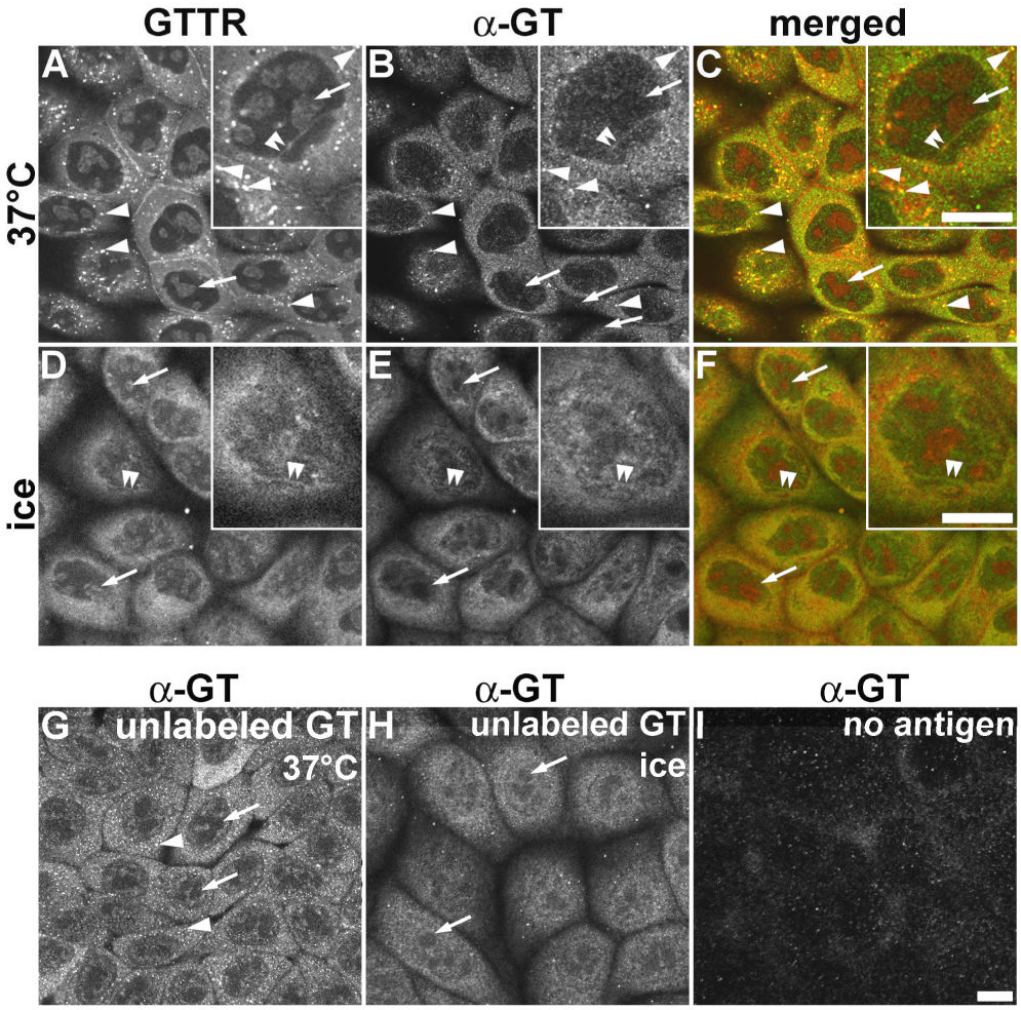

Figure 7. Immunocytochemical localization of GTTR and unconjugated gentamicin

MDCK cells were treated with 5 μg/mL GTTR (A-F), or 300 μg/mL unconjugated gentamicin (G,H) for 2 hours, fixed with FA only, permeabilized with methanol, and immunolabeled. A) In cells incubated at 37°C, GTTR fluorescence occurs as both diffuse and punctate (arrowheads) cytoplasmic labeling, with labeled nucleoli (arrows, and inset) and trans-nuclear tubules (double arrowheads, inset). B) Gentamicin immunolabeling of GTTR seen in (A) also reveals diffuse cytoplasmic, and intracellular puncta (arrowheads) of labeling; with weak labeling of the nucleoplasm, and labeled trans-nuclear tubules (double arrowheads, inset). GTTR-labeled nucleoli are not immunolabeled (arrows). C) Merged images of (A) and (B), show co-localization of both GTTR and immunofluorescence as yellow in the cytoplasm, puncta (arrowheads), and intra-nuclear tubules (double arrowheads). D) Cells loaded with GTTR on ice reveal very few intracellular puncta of fluorescence (compared to A), and robust, diffuse cytoplasmic and weak nucleoplasmic labeling, with labeled trans-nuclear tubules (double arrowheads) and nucleoli (arrows, inset). E) Gentamicin immunolabeling (α-GT) of GTTR seen in (A) also reveals only diffuse cytoplasmic and nucleoplasmic labeling, with weakly labeled trans-nuclear tubules (double arrowheads, inset). GTTR-labeled nucleoli are not immunolabeled (arrows). F) Merged image of (D) and (E). G) Immunofluorescence of gentamicin-loaded cells incubated at 37°C ice reveals diffuse cytoplasmic and nucleoplasmic labeling, intracellular fluorescent puncta (arrowheads). Presumptive sites of nucleoli are not immunolabeled (arrows). H) Immunofluorescence of gentamicin-loaded cells incubated on ice

reveals diffuse cytoplasmic and nucleoplasmic labeling, with few intracellular puncta of fluorescence. Presumptive GTTR-labeled intra-nuclear structures are not immunolabeled (arrows). I) Cells, without gentamicin or GTTR treatment, incubated on ice and immunoprocessed with primary and secondary IgG display negligible non-specific labeling. Scale bars = 10 μm.